Emergence and stability of intermediate open vesicles in disk-to-vesicle transitions

Jianfeng Li,* Hongdong Zhang, and Feng Qiu
The State Key Laboratory of Molecular Engineering of Polymers, Department of Macromolecular Science, Fudan University, Shanghai 200433, China

An-Chang Shi†
Department of Physics and Astronomy, McMaster University, Hamilton, Ontario, Canada L8S 4M1
(Received 22 February 2012; published 17 July 2013)

The transition between two basic structures, a disk and an enclosed vesicle, of a finite membrane is studied by examining the minimum energy path (MEP) connecting these two states. The MEP is constructed using the string method applied to continuum elastic membrane models. The results reveal that, besides the commonly observed disk and vesicle, open vesicles (bowl-shaped vesicles or vesicles with a pore) can become stable or metastable shapes. The emergence, stability, and probability distribution of these open vesicles are analyzed. It is demonstrated that open vesicles can be stabilized by higher-order elastic energies. The estimated probability distribution of the different structures is in good agreement with available experiments.

DOI: 10.1103/PhysRevE.88.012719 PACS number(s): 87.16.D−, 87.16.A−

I. INTRODUCTION

Amphiphilic molecules such as lipids, surfactants, and block copolymers dissolved in water can form various structured aggregates including spherical and cylindrical micelles, disklike membranes, as well as open and closed vesicles [1–4]. The formation of, and transition between, these fascinating structures have attracted tremendous attention [1–12]. In particular, the disk-to-vesicle transition has been recently examined experimentally and theoretically [13–21], motivated by the rich physics contained in this simple system, as well as by its biological implications and potential applications in drug delivery [13,22].

It is generally believed that the competition between the line tension of membrane edge and the bending rigidity of the membrane dictates most of these shape transitions [1]. In particular, the disk-to-vesicle transition presents a paradigm for the study of the competition between edge energy and bending energy of a finite membrane. When the edge energy or line tension is large, closed vesicles that minimize the edge energy at the cost of bending energy prevail, whereas the disks, which minimize the bending energy at the cost of edge energy, dominate the small line tension region. It is widely accepted that there is no metastable (or stable) intermediate along the disk-to-vesicle transition. However, previous experiments [13, 23,24] have revealed that intermediate open vesicles, in the form of vesicles with small pores or bowl-shaped structures, can be metastable or even stable. It is therefore desirable to revisit the disk-to-vesicle transition to understand and resolve this discrepancy.

In general, two major theoretical challenges for the study of membrane deformation are as follows: (1) predicting the equilibrium membrane shapes analytically or numerically (e.g., Refs. [1,8,9]), and (2) obtaining transition pathways connecting the different equilibrium shapes (e.g., Ref. [25]). In the current study, we focus on transition pathways connecting the two simplest shapes, i.e., disk and vesicle, of a finite membrane. In the context of the classic continuum elastic membrane model [8–10], this transition has been previously studied either by solving the shape equations [9] to obtain the minima (or maxima) along the transition pathway, or by assuming some particular intermediate shapes along the transition pathways to examine the transitions between the different shapes [5–7,26]. For the disk-to-vesicle transition, solving the shape equations of an open membrane with a free edge is a highly nontrivial problem. The free-boundary shape equation related to open membranes has been studied by a large number of researchers [26–30]. Recently, Umeda *et al.* [20] applied the Tu and Ou-Yang's method [28,29] to the disk-to-vesicle transition. By including the area difference between the two monolayers, or leaflets, of the bilayer membrane energy into the Helfrich energy, they obtained various metastable or stable intermediate open vesicles. Therefore, they had resolved, to some extent, the problem of missing metastable intermediate states observed in the experiments [13,23,24]. On the other hand, the solutions of the shape equation correspond to the minima or maxima of the energy landscape. Information about the transition pathway itself, which connects these extrema, is still missing. A previous study of the transition pathway is carried out by assuming that the intermediate shapes of the membrane are a series of spherical caps [5–7,26]. This spherical-cap model (SCM) essentially assumes that the reaction coordinate of the disk-to-vesicle transition is specified by the spherical caps. This simple model captures some important features of the disk-to-vesicle transition. However, this SC model failed to predict the metastable intermediate states observed in experiments. Furthermore, within the framework of the Helfrich model, Tu [31] proved that the spherical cap cannot be a stable open vesicle, thus it is desirable to go beyond the spherical-cap approximation. It should also be noticed that most of the theoretical studies of membrane shape transitions are based on the linear elastic (Helfrich) model, in which the contribution from the higher-order terms of the bending energy is neglected. On the other hand, recent experiments and theoretical analysis [32–35] have demonstrated that the higher-order contributions to the elastic bending energy of bilayer

*lijf@fudan.edu.cn
†shi@mcmaster.ca

membranes can be significant and thus cannot be ignored under certain circumstances. In particular, it is important to examine whether the higher-order blending energy contributions could stabilize some intermediate states.

The key to thoroughly understand the disk-to-vesicle transition is to construct the most probable transition pathway connecting the two structures. According to large deviation theory, the most probable transition path connecting two stable states is a minimum energy path (MEP) of the free-energy (F) landscape of the system. Mathematically, a MEP is a one-dimensional path, ϕ, in the configuration space, which is characterized by a vanishing normal component of the free-energy gradient on the path, $(\nabla F)^{\perp}(\phi) = 0$. Geometrically, the MEP can be viewed as a one-dimensional curve or string in the configuration space [36]. Specifically for the disk-to-vesicle transition, a MEP is a string in the shape space connecting the disk and vesicle states. It has been shown that the MEP can be computed using a dynamical evolution method, or the string method [36,37]. The string method has been proven to be an effective technique for the construction of MEPs in various systems including membrane adhesion [38], capillary condensation [39], vesicle pore formation [40], and phase transitions of block copolymers [41,42]. In the current work, the MEP of the disk-to-vesicle transition is constructed using the string method applied to the elastic membrane model of symmetric bilayers [43]. The MEP provides full information about the transitions between the two stable states, including intermediate metastable or stable open membrane shapes. Furthermore, the MEP can be used to estimate the probability distribution of these intermediates.

II. METHODOLOGY

In the classical continuum membrane model [8–10], a bilayer membrane is modeled by a smooth surface [44]. For the disk-to-vesicle transition, the free energy of an open membrane consists of the bending energy of the surface (S) and the edge energy of the open boundary (∂S),

$$F = \int_S \left(\frac{\kappa}{2}H^2 + \kappa_G K + \kappa_1 H^4 + \kappa_2 K^2 + \kappa_3 H^2 K\right) dA + \int_{\partial S} \gamma\, dl, \tag{1}$$

where γ is the line tension, H the mean curvature, and K the Gaussian curvature. κ, κ_G, and κ_i are the bending, Gaussian, and fourth-order moduli, respectively. It should be noticed that the commonly used Helfrich energy only contains terms up to the second order [8]. The higher-order terms are kept here for generality [32–35]. We will also examine their effects on the stability of the intermediate open vesicles. In the parallel surface model, the higher-order terms come from Taylor expansion of the bilayer energy [45]. Since only symmetrical bilayer membranes are considered [43], odd-order terms are excluded in F. For simplicity, the membrane shape is assumed to be axisymmetric and the membrane area is kept constant during the transformation. Under these assumptions, the free energy of the membrane can be cast in the configuration space specified by the variable $\phi = [r(s), \partial z(s)/\partial s]$, where s ($s \in [0,1]$) is a parameter with $s = 0$ corresponding to the bottom point and $s = 1$ the edge point of the membrane. The variables $r(s)$ and $z(s)$ measure the distances from the point s to the axial and bottom plane of the membrane, respectively [Fig.1(II)]. In terms of ϕ, the area element, mean, and Gaussian curvatures can be expressed as $dA = 2\pi r(r'^2 + z'^2)^{1/2} ds$, $H = c_1 + c_2$, and $K = c_1 c_2$, with the two principal curvatures specified by

$$c_1 = \frac{-z'}{r\sqrt{r'^2 + z'^2}}, \tag{2}$$

$$c_2 = \frac{r''z' - r'z''}{(r'^2 + z'^2)^{3/2}}, \tag{3}$$

where the derivatives with respect to the variable s are denoted by $X' \equiv \partial X/\partial s$. The string method of MEP starts from an initial string, $\phi(s,\alpha;t)|_{t=0}$, which is parametrized by a variable α ($\alpha \in [0,1]$) such that $\alpha = 0$ corresponds to the disk and $\alpha = 1$ the vesicle. This string variable α can be taken as the radius of the open edge, $\alpha = 1 - r(1)/R_0$. In order to obtain the MEP, the initial string is evolved according to the dissipative dynamic equation [36,37],

$$\frac{\partial \phi}{\partial t} = -(\nabla F)(\phi) + \eta\vec{\tau} + \lambda\vec{v}, \tag{4}$$

where $\vec{\tau}$ is the unit tangent vector of ϕ defined by $\vec{\tau} = \partial_\alpha\phi/|\partial_\alpha\phi|$ with $\partial_\alpha\phi \equiv \partial\phi/\partial\alpha$, $|\partial_\alpha\phi| \equiv \sqrt{\int(\partial_\alpha\phi)^2 dA}$, and $\vec{v} = (r', z')$. The Lagrange multiplier η is determined by the parametrization of the string, while λ ensures a constant membrane area. In practice, explicit evaluation of the Lagrange multiplier η is not required in the numerical implementation. Instead an equal arc length parametrization of the string is enforced by using the interpolation method proposed by E *et al.* [37]. The gradient of the energy landscape $(\nabla F)(\phi)$ is evaluated numerically based on the discrete variational principles [46,47] (see the Appendix). A string is represented by 100 structures or 100 shapes in the configuration space. The initial string is taken as a series of spherical caps. Furthermore, each shape in the calculation is represented by 90 discrete points, or the variable s is discretized into 89 segments. The MEP of the transition is obtained when the evolution equation reaches a steady state, $\phi(s,\alpha)_{\mathrm{MEP}} = \phi(s,\alpha;t)|_{t=\infty}$. In what follows we present results on the disk-to-vesicle MEPs for two models, the linear Helfrich model with $\kappa_1 = \kappa_2 = \kappa_3 = 0$, and the nonlinear Helfrich model with some specific choices of nonzero κ_1, κ_2, and κ_3. These MEPs are then used to search for stable and metastable intermediate states. The probability of finding these intermediates (bowl-like membranes and vesicles with small pore) is estimated by noticing that, with the availability of the MEP, the probability of finding a membrane shape with string parameter α is proportional to $\exp\{-F(\alpha)/k_B T\}$ with $F(\alpha)$ the free energy of the MEP.

III. RESULTS

We first examine the case of the linear Helfrich model with $\kappa_1 = \kappa_2 = \kappa_3 = 0$ [Eq. (1)]. Since the energy can be scaled by the bending modulus κ, the results are shown with a fixed κ and varying γ and κ_G (Fig. 1). The first obvious result from the MEP shown in Fig. 1 is that the spherical cap model [48] overestimates the MEP and spherical caps are

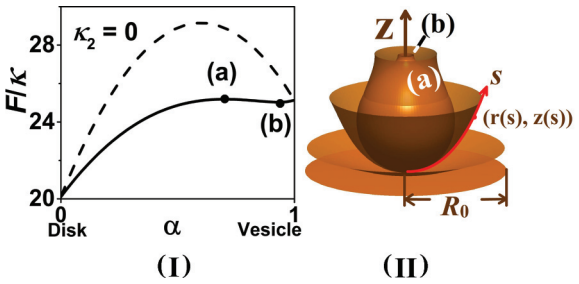

FIG. 1. (Color online) A typical MEP for $\kappa_i = 0$. (I) Free energy (solid line) of the MEP at $\frac{\gamma R_0}{4\kappa} = 0.8$ and $\kappa_G = 0$. The dashed line is obtained by the spherical-cap model. (II) Five representative shapes along the MEP with (a) corresponding to the maximum and (b) to the metastable vesicle pore on the MEP. These five are at $\alpha = 0$, 0.03, 0.25, 0.70, 0.93, respectively.

clearly not representation of the intermediates on the MEP. Indeed, we have numerically shown that a spherical cap is not a stable shape along the transition, in agreement with the earlier study of Tu [31] within the framework of the Helfrich model. Furthermore, the string method predicts a metastable open vesicle with a small pore along the transition. The depth of the potential well is about $0.06\kappa \approx 1.8 k_B T$ if we take $\kappa = 1.2 \times 10^{-19}$ J and $\gamma R_0/4\kappa = 0.8$ [13]. This metastable intermediate may correspond to the transient vesicle pores observed in the viscous solutions by Saito *et al.* [23]. Metastable open vesicles have been also obtained by solving the shape equations (see Umeda *et al.* [20]). The shape phase diagram of the transition can be constructed by examining the extrema of the MEP (Fig. 2). It is observed that the metastable vesicles with a small pore exist only in a small region labeled "D + Pore" shown in Fig. 2. The phase boundary between "D + V" and "V" defines the critical line tension of the disk, beyond which the disk becomes absolutely unstable and it will transform into vesicle spontaneously. For the linear Helfrich model, this phase boundary can be obtained analytically by solving the free-boundary shape equations and it is determined by a transcendental equation [28],

$$2\tilde{\gamma}_c^{1/2} J_0\left(2\tilde{\gamma}_c^{1/2}\right) / J_1\left(2\tilde{\gamma}_c^{1/2}\right) = -\kappa_G/\kappa, \tag{5}$$

where J_0 and J_1 are the zeroth- and first-order Bessel functions of the first kind, and $\tilde{\gamma} = \gamma R_0/4\kappa$ is the reduced line tension. Clearly, the critical value depends on the Gaussian modulus κ_G.

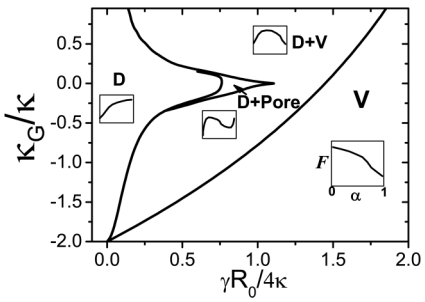

FIG. 2. (κ_G,γ) phase diagram for $\kappa_i = 0$ showing the stability region of different shapes with the corresponding MEP schematics. The stable or metastable shapes are indicated by "D" (disk), "V" (vesicle), and "pore" (vesicle with a pore with $\alpha > 0.5$). The insets illustrate the energy profile in each phase region.

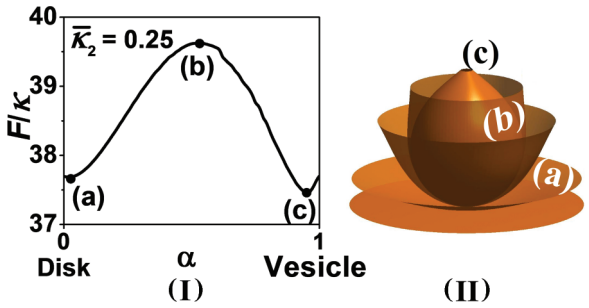

FIG. 3. (Color online) A typical MEP for $\kappa_2 \neq 0$ and $\kappa_1 = \kappa_3 = 0$. Left: Free energy of the MEP at $\frac{\gamma R_0}{4\kappa} = 1.8$ and $\frac{\kappa_2}{\kappa R_0^2} = 0.25$. Right: Five typical shapes on the MEP showing in (I) at $\alpha = 0$, 0.03, 0.25, 0.53, 0.95. Shape (b) corresponds to the maximum of the MEP, while the bowl-like membrane (a) and vesicle with a pore (c) are the metastable and stable states, respectively.

In particular, when $\kappa_G = 0$, $\tilde{\gamma}_c = 1.445$. In agreement with this exact result, the string method gives $\tilde{\gamma}_c = 1.44$. On the other hand, the spherical cap model (SCM) [26] predicts $\tilde{\gamma}_c = 2$.

For the case of the nonlinear membrane model with a particular choice of $\kappa_1 = \kappa_3 = 0$ and $\kappa_2 \neq 0$ [Eq. (1)], the transition behavior becomes more complex. Figures 3(I) and 3(II) show the MEP and several open membrane shapes at $\kappa_2/R_0^2\kappa = 0.25$ and $\tilde{\gamma} = 1.5$. It is interesting to notice that, with this set of model parameters, the MEP predicts the existence of a metastable bowl-like membrane and a stable vesicle with a small pore. The difference between the minimum energies corresponding to these two intermediates is small, indicating that they may coexist under some conditions (also see Fig. 5). The shapes of these open membranes are obviously different from those of the linear case ($\kappa_2 = 0$, Fig. 1). In the case of the linear membrane model, the membrane edges tend to curl up ($c_2 > 0$) because the membranes tend to maintain a zero mean curvature near the edge. For the nonlinear model, the membrane edges are more straight ($c_2 \approx 0$) because of the energetic penalty of $\kappa_2 K^2$. This phenomenon can be better understood by examining one of the boundary conditions in the free-boundary shape equations [28],

$$[\kappa(c_1 + c_2) + c_1(\kappa_G + 2\kappa_2 c_1 c_2)]_{s=1} = 0. \tag{6}$$

As can be seen from this boundary condition at the open edge, for the linear case we have $c_2 = -(\kappa + \kappa_G)c_1/\kappa > 0$, because the principal curvature c_1 perpendicular to the axial direction is mostly negative. Note that $c_2 > 0$ corresponds to a curling-up edge while $c_2 = 0$ leads to a straight edge (along the axial direction). Therefore a negative Gaussian modulus tends to flatten the edge (in particular, $c_2 = 0$ if $\kappa_G = -\kappa$); this phenomenon has been also noticed by Yao *et al.* [12]. For the nonlinear case, $c_2 = -(\kappa + \kappa_G)c_1/(\kappa + \kappa_2 c_1^2)$, implying that the principal curvature c_2 will be small for a large κ_2, i.e., a big κ_2 will also flatten the membrane edge. It is interesting to point out that the membrane shapes observed in the experiments [13] are closer to those of the nonlinear case ($\kappa_2 \neq 0$), implying that the higher-order curvature energies may contribute significantly in this case. Also by comparing these shapes, we have confirmed in theory that the experimentally observed intermediates mostly follow the MEPs. More results

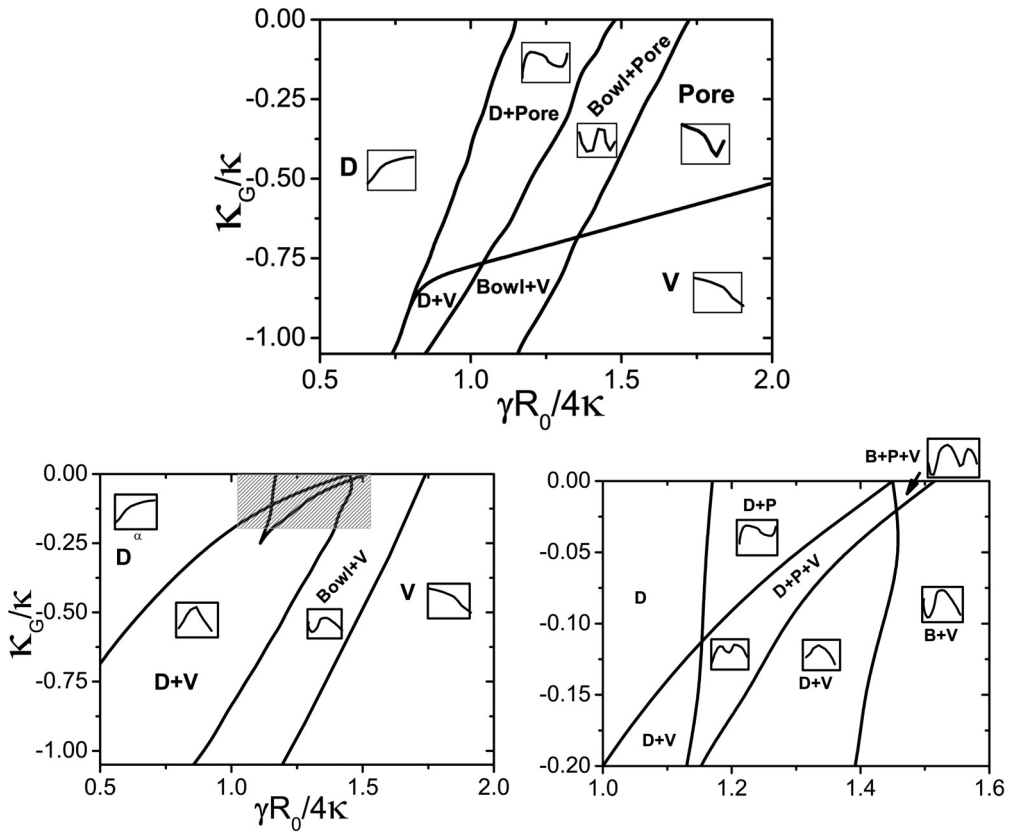

FIG. 4. Upper: (κ_G,γ) phase diagram at $\frac{\kappa_2}{\kappa R_0^2} = 0.25$ and $\kappa_1 = \kappa_3 = 0$. Lower: The phase diagram at $\frac{16\kappa_1}{\kappa R_0^2} = 0.25$ and $\kappa_2 = \kappa_3 = 0$; a zoom-in view of the shadow region of the phase diagram is shown on the lower left. The stable or metastable shapes are indicated by "D" (disk), "V" (vesicle), "pore" (vesicle with a pore with $\alpha > 0.5$), and "Bowl" ($\alpha < 0.5$). The insets illustrate the energy profile in each phase region.

of the present case are summarized in the phase diagram (the upper panel in Fig. 4). The MEP depicted in Fig. 3 corresponds to a point in the phase region "Bowl + Pore." Besides "Bowl + Pore" some bowl-like membranes in the "Bowl + V" region are stable while vesicles with the pore in the "Pore" are stable. Although the theory predicts the existence of open vesicles as stable and metastable states of a finite membrane, care must be taken when making direct comparison of the phase diagram shown in Fig. 4 with experiments. For example, the reduced Gaussian modulus (κ_G/κ) of lipid membranes is normally about -1, while the phase diagram of Fig. 4 predicts that open vesicles with a small pore can be stable for $\kappa_G/\kappa > -0.75$ with $\kappa_2/\kappa R_0^2 = 0.25$. On the other hand, it is interesting to notice that the Gaussian modulus κ_G can be mediated by the spontaneous curvature of the monolayer [45]. In order to make a detailed comparison with experiments, accurate values of the elastic moduli are desirable.

The effects of the other nonlinear terms have been also examined by computing the MEPs for nonzero κ_1. The results (see the lower panels in Fig. 4) reveal that the $\kappa_1 H^4$ term has a similar effect as that of the κ_2 term. That is, a positive κ_1 will stabilize the bowl-like membranes. On the other hand, for the cases of a negative κ_1 or a negative κ_2 or any nonvanishing κ_3 alone (with $\kappa_1 = \kappa_2 = 0$), a smooth membrane would not be stable because the higher-order energy terms of these three cases are not positive definite. In general, the positive-definite condition is $\kappa_1 + \kappa_2 \geqslant 0$ and $4\kappa_1\kappa_2 \geqslant \kappa_3^2$, and there are many combinations of κ_1, κ_2, and κ_3 satisfying the positive-definite conditions. For a given set of the higher-order modulus, it is straightforward to examine their transition pathways using the string method.

An estimation of the probability distribution function (PDF) of the intermediate states requires the knowledge of the entire transition pathway. To match the experiment parameters [13], we set $\kappa = 1.2 \times 10^{-19}$ J, $\kappa_G = 0$, $R_0 = 10$ μm, and $\kappa_2/R_0^2\kappa = 0.25$; the value of γ obeys the normal distribution with a standard deviation $\Delta\gamma = 0.02$ pN. We explore three typical mean line tensions, 0.062, 0.094, and 0.12 pN, respectively (the corresponding $\tilde{\gamma}$'s are 1.29, 1.96, and 2.5). The PDFs are shown in the lower panels of Fig. 5. Based on these PDFs, the probabilities of finding the four typical shapes (disk, bowl, vesicle with a pore, and closed vesicle) are integrated and presented in the upper panels. For a large value of γ (0.12 pN), almost no open membranes are observed. As the line tension is decreased from 0.094 to 0.062 pN, the percentage of the open membranes is predicted to rise from 17.1% to 73.2%. These results are consistent with a recent experiment [13], in which photosensitive molecules (KAON12) are used to reduce the line tension of the membrane in order to stabilize bowl-like and cuplike membranes.

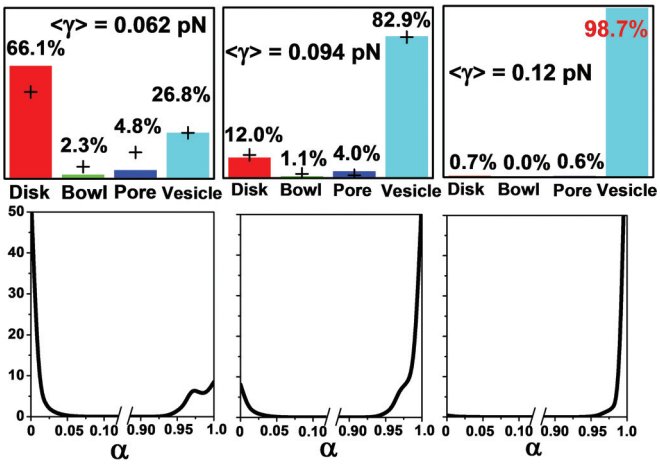

FIG. 5. (Color online) Upper: Probabilities of finding the disks ($\alpha < 0.03$), bowls ($0.03 < \alpha < 0.5$), vesicles with a pore ($0.5 < \alpha < 0.96$), and vesicles ($\alpha > 0.96$) in the solution of lipids, estimated by the string method. The + data points are taken from Fig. 2 in Ref. [13], with $\langle\gamma\rangle = 0.062$ pN corresponding to the case of 40% KAON12 and 0.094 pN to 35% KAON12, respectively. Lower: The PDFs corresponding to the upper ones.

For simplicity, our calculations were carried out for the cases with zero spontaneous curvature. For membranes with nonzero spontaneous curvatures, it is expected that intermediate open vesicles may become stable states, similar to the cases of area-difference models studied by Umeda *et al.* [20], which exhibit stable open vesicles under certain conditions. In the current work we focus on the methodology of finding the transition pathways between the disk and vesicle states and the effect of the higher-order elastic bending terms, and we leave the case of nonzero spontaneous curvature to a future study.

IV. CONCLUSION

In summary, we have examined the disk-to-vesicle transitions of finite membranes by constructing the minimum energy path (MEP) connecting these two states. Specifically, the MEPs are obtained by applying the string method to the classical linear and nonlinear elastic membrane models. Membrane shapes along the MEP are used to predict transition pathways and intermediate states from disks to vesicles. The minima along the MEP correspond to stable and metastable intermediate states between the disks and vesicles. The predicted intermediate shapes, in the form of a bowl-like shape and a vesicle with a small pore, along the transition pathways are in good agreement with the experimentally observed intermediates. In the case of the linear elastic (Helfrich) model, only metastable open vesicles with a small pore are predicted by the MEP. When nonlinear elastic curvature energy is included in the membrane model, both stable bowl-shaped membranes and vesicles with a small hole are obtained. These intermediate open structures can be stabilized by nonlinear elastic terms in the membrane energy. Finally, the MEP can be used to estimate the probability distribution of the different intermediate states. The predicted shape sequence along the MEP can be used to understand the nature of disk-to-vesicle transitions of open membranes. Furthermore, although the method is developed for the disk-to-vesicle transition, in principle it can be applied to the study of the transitions among other two-dimensional structures, such as vesicles with many pores and membrane tubes or torus. Finally, we would like to emphasize that, since the theory is based on the continuum elastic model of membranes, the results are relevant to generic amphiphilic systems such as lipids and surfactants.

ACKNOWLEDGMENTS

We are grateful to the support from the National Basic Research Program of China (Grant No. 2011CB605700), the National Natural Science Foundation of China (Grants No. 20990231 and No. 21104010), and the Natural Science and Engineering Research Council (NSERC) of Canada. The computation was made possible by the facilities of the Shared Hierarchical Academic Research Computing Network (SHARCNET: www.sharcnet.ca).

APPENDIX: EVALUATION OF THE GRADIENT $(\nabla F)(\phi)$

In this Appendix we provide some details of the numerical procedures to evaluation of the functional gradient of the free energy $(\nabla F)(\phi)$. Mathematically $(\nabla F)(\phi)$ is the variational derivative of the free energy F with respect to the variable ϕ. For an open membrane with rotational symmetry about the z axis, a naive discretization of the space will encounter a singularity at the central bottom point ($z = r = 0$). Furthermore, care must be taken to treat the boundary condition at the free edge of the membrane.

Based on the discrete variational principle [46,47], a discretization scheme can be developed for the open membrane problem. This scheme preserves the symmetry of the free-energy functional. With this scheme, the singularity at the bottom of the membrane can be removed by a proper formulation of the discrete free-energy density at this point and the boundary conditions at the free edge are automatically satisfied. In our numerical calculations, we discretize the free energy (action) first and then perform the variation of the *discrete* energy to obtain the discrete gradient $(\nabla F)(\phi)$. This procedure ensures that the symmetry of the system is preserved. Symmetric schemes also lead to better numerical stability.

For an axisymmetric open membrane, its shape is described by the position of the membrane $R(s) = [r(s), z(s)]$. In the discretized description, the membrane shape is represented by $\mathbf{R}(k) = [r(k), z(k)]$ with $k = 0, 1, \ldots, N$. It is convenient to define the following variables,

$$\zeta(k) \equiv [z(k) - z(k-1)]/\Delta s,$$
$$r_s(k) \equiv [r(k) - r(k-1)]/\Delta s,$$
$$\zeta_s(k) = [\zeta(k) - \zeta(k-1)]/\Delta s.$$

These quantities near the bottom point (i.e., $k = -1, 0, 1$) are specified by the following symmetric scheme,

$$r(0) = 0, \quad z(0) = 0, \quad z(-1) = z(1),$$
$$r(-1) = -r(1), \quad r_s(0) = 0, \quad \zeta(0) = 0.$$

The length element $\sqrt{r'^2 + z'^2}$, area element dA, and curvature of the membrane can be expressed in terms of these

discretized variables,

$$
\begin{aligned}
D(k) &= \{[r(k+1)-r(k-1)]^2 \\
&\quad + [z(k+1)-z(k-1)]^2\}^{1/2}/2\Delta s, \\
S(k) &= \{[3r(k)+r(k-1)]d(k) \\
&\quad + [3r(k)+r(k+1)]d(k+1)\}\Delta s/8, \\
c_1(k) &= -\frac{\zeta(k)+\zeta(k+1)}{2r(k)D(k)}, \\
c_2(k) &= \frac{[\zeta(k)r_s(k+1)-\zeta(k+1)r_s(k)]}{d(k)d(k+1)D(k)\Delta s},
\end{aligned}
$$

where $d(k) = [r_s(k)^2 + \zeta(k)^2]^{1/2}$. The curvatures at the bottom point are specified by $c_1(0) = c_2(0) = -2\zeta(1)/d(1)^2$. It should be noticed that, although the variables $r_s(k)$ and $\zeta(k)$ are not symmetric about k, the discrete expressions of the area element and principal curvatures are symmetric about k. The discretization of c_1 is obtained by *interpolating* the three points $k-1$, k, and $k+1$ with an arc and then calculating the corresponding inverse radius as the principal curvature. The mean curvature and Gaussian curvature are expressed in terms of c_1 and c_2, i.e., $H = c_1 + c_2$ and $G = c_1c_2$. Finally the energy functional F is obtained in terms of these discretized variables,

$$
F = \sum_{k=0}^{k=N-1} 2\pi f(H,K)S(k) + 2\pi\gamma r(N), \tag{A1}
$$

where $f(H,K) = \frac{\kappa}{2}H^2 + \kappa_G K + \kappa_1 H^4 + \kappa_2 K^2 + \kappa_3 H^2 K$.

The expression of the discretized energy functional [Eq. (A1)] allows the numerical calculation of the discrete variational derivatives [49],

$$
\frac{\delta F}{\delta r(k)} = \lim_{a\to 0}\frac{F[r(k)+a]-F[r(k)]}{a}, \tag{A2}
$$

$$
\frac{\delta F}{\delta \zeta(k)} = \lim_{a\to 0}\frac{F[\zeta(k)+a]-F[\zeta(k)]}{a}, \tag{A3}
$$

where a is a sufficiently small real number and $k = 0,1,\ldots,N$.

It should be noticed that the discrete variational derivative can be obtained analytically from the energy functional,

$$
\frac{\delta F}{\delta r(k)} = \frac{\partial F(r(1),r(2),\ldots,r(N))}{\partial r(k)}, \tag{A4}
$$

with a similar expression for $\delta F/\delta\zeta(k)$. In practice, obtaining explicit expressions of these derivatives are quite tedious. In our calculations we employed the numerical variation scheme [Eqs. (A2) and (A3)] to calculate these functional derivatives.

Finally we would like to point out that the boundary conditions at the free edge are automatically satisfied in our discretization expressions. Specifically the derivatives at the free edge are given by $\delta F/\delta r(N-1) = 0$, $\delta F/\delta r(N) = 0$, and $\delta F/\delta\zeta(N) = 0$, corresponding to the three boundary conditions in the shape equations of open membranes [20,27–29].

[1] R. Lipowsky and E. Sackmann, *Structure and Dynamics of Membranes* (Elsevier, Amsterdam, 1995).
[2] S. Šegota and D. Težak, Adv. Colloid Interface Sci. **121**, 51 (2006).
[3] E. W. Kaler, A. K. Murthy, B. E. Rodriguez, and J. A. N. Zasadzinski, Science **245**, 1371 (1989).
[4] M. Gradzielski, Curr. Opin. Colloid Interface Sci. **16**, 13 (2011).
[5] D. D. Lasic, Biochim. Biophys. Acta **692**, 501 (1982).
[6] P. Fromherz, Chem. Phys. Lett. **94**, 259 (1983).
[7] D. D. Lasic, Biochem. J. **256**, 1 (1988).
[8] W. Helfrich, Z. Naturforsch. C **28**, 693 (1973).
[9] O.-Y. Zhong-can and W. Helfrich, Phys. Rev. A **39**, 5280 (1989).
[10] U. Seifert, K. Berndl, and R. Lipowsky, Phys. Rev. A **44**, 1182 (1991).
[11] S. Svenson, Curr. Opin. Colloid Interface Sci. **9**, 201 (2004).
[12] Z. Yao, R. Sknepnek, C. K. Thomas, and M. Olvera de la Cruz, Soft Matter **8**, 11613 (2012).
[13] T. Hamada, R. Sugimoto, M. C. Vestergaard, T. Nagasaki, and M. Takagi, J. Am. Chem. Soc. **132**, 10528 (2010).
[14] M. P. Nieh, V. A. Raghunathan, S. R. Kline, T. A. Harroun, C. Y. Huang, J. Pencer, and J. Katsaras, Langmuir **21**, 6656 (2005).
[15] B. Deme, M. Dubois, T. Gulik-Krzywicki, and T. Zemb, Langmuir **18**, 997 (2002).
[16] J. Leng, S. U. Egelhaaf, and M. E. Cates, Biophys. J. **85**, 1624 (2003).
[17] J. Gummel, M. Sztucki, T. Narayana, and M. Gradzielski, Soft Matter **7**, 5731 (2011).
[18] G. J. A. Sevink and A. V. Zvelindovsky, Macromolecules **38**, 7502 (2005).
[19] X. He and F. Schmid, Phys. Rev. Lett. **100**, 137802 (2008).
[20] T. Umeda, Y. Suezaki, K. Takiguchi, and H. Hotani, Phys. Rev. E **71**, 011913 (2005).
[21] W. Shinoda, T. Nakamura, and S. O. Nielsen, Soft Matter **7**, 9012 (2011).
[22] T. M. Allen and P. R. Cullis, Science **303**, 1818 (2004).
[23] A. Saitoh, K. Takiguchi, Y. Tanaka, and H. Hotani, Proc. Natl. Acad. Sci. USA **95**, 1026 (1998).
[24] F. Nomura, M. Nagata, and T. Inaba, Proc. Natl. Acad. Sci. USA **98**, 2340 (2001).
[25] H. W. G. Lim, M. Wortis, and R. Mukhopadhyay, Proc. Natl. Acad. Sci. USA **99**, 16766 (2002).
[26] D. H. Boal and M. Rao, Phys. Rev. A **46**, 3037 (1992).
[27] R. Capovilla, J. Guven, and J. A. Santiago, Phys. Rev. E. **66**, 021607 (2002).
[28] Z. C. Tu and Z. C. Ou-Yang, Phys. Rev. E **68**, 061915 (2003).
[29] Z. C. Tu and Z. C. Ou-Yang, J. Phys. A: Math. Gen. **37**, 11407 (2004).
[30] Y. Yin, J. Yin, and D. Ni, J. Math. Biol. **51**, 403 (2005).
[31] Z. C. Tu, J. Chem. Phys. **132**, 084111 (2010).
[32] M. I. Katsnelson and A. Fasolino, J. Phys. Chem. B **110**, 30 (2006).
[33] O. V. Manyuhina *et al.*, Phys. Rev. Lett. **98**, 146101 (2007).
[34] O. V. Manyuhina, J. J. Hetzel, M. I. Katsnelson, and A. Fasolino, Eur. Phys. J. E **32**, 223 (2010)

[35] J. F. Li, K. A. Pastor, A.-C. Shi, F. Schmid, and J. J. Zhou, Phys. Rev. E **88**, 012718 (2013).
[36] W. E, W. Ren, and E. Vanden-Eijnden, Phys. Rev. B **66**, 052301 (2002).
[37] W. E, W. Ren, and E. Vanden-Eijnden, J. Chem. Phys. **126**, 164103 (2007).
[38] C.-Z. Zhang and Z.-G. Wang, Phys. Rev. E **77**, 021906 (2008).
[39] C. Qiu, T. Qian, and W. Ren, J. Chem. Phys. **129**, 154711 (2008).
[40] C. L. Ting, D. Appelo, and Z.-G. Wang, Phys. Rev. Lett. **106**, 168101 (2011).
[41] L. Lin, X. Cheng, W. E, A.-C. Shi, and P. Zhang, J. Comput. Phys. **229**, 1797 (2010).
[42] X. Cheng, L. Lin, W. E, P. Zhang, and A.-C. Shi, Phys. Rev. Lett. **104**, 148301 (2010).
[43] A symmetrical bilayer is referred to as a bilayer with the identical chemical compositions and zero area difference about its two leaflets. Because the chemicals can diffuse across the membrane edge, therefore in the long term the bilayer will eventually become symmetrical.
[44] The continuum membrane theory cannot, in principle, consider the lipid rearrangements or membrane fusions related to vesicle pore formations. Luckily, the rearrangement process in the vesicle pore formation has been recently studied by the string method applied to the self-consistent field theory [40].
[45] U. S. Schwarz and G. Gompper, Langmuir **17**, 2084 (2001).
[46] J. E. Marsden and M. West, Acta Numer. **10**, 357 (2001)
[47] J. F. Li, H. D. Zhang, P. Tang, F. Qiu, and Y. L. Yang, Macromol. Theory Simul. **15**, 432 (2006).
[48] The free energy of the spherical cap model can be expressed in terms of the edge angle θ as $4\pi[(1+\kappa_G/\kappa)(1-\cos\theta)+2\bar{\gamma}\sin\theta/\sqrt{2-2\cos\theta}]$ with $\bar{\gamma}=\gamma R_0/4\kappa$.
[49] K. A. Brakke, Exp. Math. **1**, 141 (1992).